

Effect of Three-Phase Contact Line Topology on Dynamic Contact Angles on Heterogeneous Surfaces

Neeharika Anantharaju,[†] Mahesh V. Panchagnula,^{*,†} Srikanth Vedantam,[‡]
Sudhakar Neti,[§] and Svetlana Tatic-Lucic^{||}

Department of Mechanical Engineering, Tennessee Technological University, Cookeville, Tennessee 38501,
Department of Mechanical Engineering, National University of Singapore, Singapore 117576, and
Department of Mechanical Engineering, and Sherman Fairchild Center, Department of Electrical and
Computer Engineering, Lehigh University, Bethlehem, Pennsylvania 18015

Received July 6, 2007. In Final Form: August 14, 2007

Cassie–Baxter theory has traditionally been used to study liquid drops in contact with microstructured surfaces. The Cassie–Baxter theory arises from a minimization of the global Gibbs free energy of the system but does not account for the topology of the three-phase contact line. We experimentally compare two situations differing only in the microstructure of the roughness, which causes differences in contact line topology. We report that the contact angle is independent of area void fraction for surfaces with microcavities, which correspond to situations when the advancing contact line is continuous. This result is in contrast with Cassie–Baxter theory, which uses area void fraction as the determining parameter, regardless of the type of roughness.

Introduction

Recent studies¹ as well as SEM images of hydrophobic leaf surface microstructure have demonstrated the importance of having multiple characteristic length scales to achieve lower contact angle hysteresis. The extreme water repellency demonstrated by the lotus leaf has motivated a large body of biomimetic effort to increase the hydrophobicity of surfaces.² Mimicking the surface topography of the lotus leaf, most studies have focused on the effect of microscale polyhedral poles on the contact angle of water drops on the surface (fakir condition).³ For example, researchers have created surfaces with a uniform array of poles fabricated by photolithography techniques^{4,5} or other etching methods.⁶ A variety of surface topologies have been studied: square pillars,⁷ parallel grooves,^{8–10} and circular pillars.^{4,11} For these surfaces, the contact angles are described by the classical Cassie–Baxter theory.¹² In this context, homogeneous wetting is defined as a regime where the liquid

completely wets the solid surface, whereas heterogeneous wetting is defined as the case when air (or liquid vapor) is trapped between the sessile liquid drop and the surface. The heterogeneous wetting regime is characterized by lower contact angle hysteresis than the homogeneous wetting regime.⁷ Lower contact angle hysteresis results in higher drop mobility. For both the regimes, the system Gibbs free energy consists of the surface energies of the liquid–vapor, solid–vapor, and the solid–liquid interfaces, denoted by Γ , with the subscripts LV, SV, and SL, respectively. Neglecting line tension, the total energy of the system is written as

$$G = \Gamma_{SL}A_{SL} + \Gamma_{LV}A_{LV} + \Gamma_{SV}A_{SV} \quad (1)$$

where A represents the interfacial area. Several studies have applied the free energy balance of the liquid–solid, liquid–vapor, and solid–vapor interfacial energies^{13–17} to characterize the contact angle behavior. When the surface is covered by microscale poles between which air is trapped, the surface area in contact with the drop are the top surfaces of the poles. By substituting this in the above free energy expression and minimizing, the Cassie–Baxter equation for the apparent contact angle is obtained.¹⁸ The apparent contact angle can be shown to be the weighted average of the contact angle with air (180°) and the Young's contact angle (contact angle on a smooth surface) θ_Y ,

(11) McHale, G.; Aqil, S.; Shirtcliffe, N. J.; Newton, M. I.; Erbil, H. Y. Analysis of droplet evaporation on a superhydrophobic surface. *Langmuir* **2005**, *21* (24), 11053–11060.

(12) Cassie, A. B. D. Contact angles. *Discuss. Faraday Soc.* **1948**, *3*, 11.

(13) Chatain, D.; Lewis, D.; Baland, J. P.; Carter, W. C. Numerical analysis of the shapes and energies of droplets on micropatterned substrates. *Langmuir* **2006**, *22* (9), 4237–4243.

(14) Chaudhury, M. K.; Whitesides, G. M. Correlation between surface energy and surface constitution. *Science* **1992**, *255*, 1230–1232.

(15) Porcheron, F.; Monson, P. A. Mean-field theory of liquid droplets on roughened solid surfaces: Application to superhydrophobicity. *Langmuir* **2006**, *22* (4), 1595–1601.

(16) Nosonovsky, M.; Bhushan, B. Stochastic model for metastable wetting of roughness-induced superhydrophobic surfaces. *Microsyst. Technol.: Micro-Nanosyst.—Inform. Storage Process. Syst.* **2006**, *12* (3), 231–237.

(17) Nosonovsky, M.; Bhushan, B. Wetting of rough three-dimensional superhydrophobic surfaces. *Microsyst. Technol.: Micro-Nanosyst.—Inform. Storage Process. Syst.* **2006**, *12* (3), 273–281.

(18) Marmur, A. Wetting on hydrophobic rough surfaces: To be heterogeneous or not to be? *Langmuir* **2003**, *19*, 8343–8348.

* Corresponding author. Phone: (931) 372 6143. Fax: (931) 372 6340. E-mail: mvp@tntech.edu.

[†] Tennessee Technological University.

[‡] National University of Singapore.

[§] Department of Mechanical Engineering, Lehigh University.

^{||} Department of Electrical and Computer Engineering, Lehigh University.

(1) Gao, L.; McCarthy, T. J. The “lotus effect” explained: Two reasons why two length scales of topography are important. *Langmuir* **2006**, *22*, 2966–2967.

(2) Barthlott, W.; Neinhuis, C. Purity of the sacred lotus, or escape from contamination in biological surfaces. *Planta* **1997**, *202*, 1–8.

(3) Oner, D.; McCarthy, T. J. Ultrahydrophobic surfaces, effects of topography length scales on wettability. *Langmuir* **2000**, *16*, 7777–7782.

(4) Zhai, L.; Berg, M. C.; Cebeci, F. C.; Kim, Y.; Milwid, J. M.; Rubner, M. F.; Cohen, R. E. Patterned superhydrophobic surfaces: Toward a synthetic mimic of the Namib Desert beetle. *Nano Lett.* **2006**, *6* (6), 1213–1217.

(5) Bartolo, D.; Bouamirrene, F.; Verneuil, E.; Buguin, A.; Silberzan, P.; Moulinet, S. Bouncing or sticky droplets: Impalement transitions on superhydrophobic micropatterned surfaces. *Europhys. Lett.* **2006**, *74* (2), 299–305.

(6) Baldacchini, T.; Carey, J. E.; Zhou, M.; Mazur, E. Superhydrophobic surfaces prepared by microstructuring of silicon using a femtosecond laser. *Langmuir* **2006**, *22* (11), 4917–4919.

(7) He, B.; Lee, J.; Patankar, N. A. Contact angle hysteresis on rough hydrophobic surfaces. *Colloid Surf. A* **2004**, *248*, 101–104.

(8) Chen, Y.; He, B.; Lee, J.; Patankar, N. A. Anisotropy, in the wetting of rough surfaces. *J. Colloid Interface Sci.* **2005**, *281*, 458–464.

(9) He, B.; Patankar, N. A.; Lee, J. Multiple equilibrium droplet shapes and design criteria for rough hydrophobic surfaces. *Langmuir* **2003**, *19*, 4999–5003.

(10) Iwamatsu, M. Contact angle hysteresis of cylindrical drops on chemically heterogeneous striped surfaces. *J. Colloid Interface Sci.* **2006**, *297* (2), 772–777.

$$\cos(\theta) = (1 - f) \cos(\theta_V) + f \cos(180^\circ) \quad (2)$$

where f is the area fraction of the tops of the poles to the total projected area of the surface. For the case of periodically spaced square poles of side a separated by a distance b at centers, $f = a^2/b^2$. Similarly for the case of periodically spaced square holes of side a separated by a distance b at centers, $f = 1 - a^2/b^2$. The above equation for the contact angle dependence with the area void fraction has been extensively tested by experimental measurements for fakir droplets on poles of different cross sectional shapes and over a wide range of length scales.^{7,19} However, this theoretical development does not take into account the topology of the three-phase contact line, which has been recognized to play an important role in determining the contact angle.²⁰

The contact line under consideration is formed by the liquid–vapor interface at the solid surface at which the contact angle is measured. On a smooth homogeneous surface (see Figure 1a), the liquid–vapor interface meets the solid surface on a continuous, circular three-phase contact line. In the case of poles (see Figure 1b), this contact line is only an apparent contact line formed as a crease on the continuous liquid–vapor surface as it is folded between the poles. Strictly speaking, the *three*-phase contact line is discontinuous and in the form of square loops around the tops and edges of the wetted poles. In the case of holes (see Figure 1c), the contact line is again a real, continuous *three*-phase contact line at which advancing events occur as drop volume increases.

The Cassie–Baxter theory, which does not account for the three-phase contact line topology, has been used in predicting the contact angle dependence on the area void fraction. In addition, most contact angle measurements are performed under dynamic conditions (either advancing or receding). It is curious that an equation derived for defect-free surfaces under thermodynamic equilibrium has found empirical success when applied to dynamic contact angles.²¹

A closer observation shows that, in the case of a fakir drop (where Cassie–Baxter theory has found much of its success), the three-phase contact line actually consists of multiple loops around the tops of each pole wetted by the drop. Thus, for the case of the drop on a bed of poles, the “apparent” three-phase contact line at the advancing edge of the drop (wetted circle circumference) is discontinuous and in reality is only a fold on the drop surface (the drop shape between the poles in Figure 1b). Presumably, a continuous, advancing three-phase contact line will demonstrate a behavior different from the predictions of the Cassie–Baxter theory due to the possibility of pinning.³ We test this possibility experimentally by measuring the advancing contact angle on surfaces with square cavities as well as poles.

Experimental Section

Chemicals and Materials. In the current study, we have created specimens of varying structured “roughness” on a silicon wafer using a wet-etch process. The roughness was introduced either as periodically placed square poles or square cavities of varying characteristic roughness length scale a , viz. side of the square feature, and of varying area void fraction, f (See Figure 2a,b for SEM images of two of the specimens with “holes” type and “poles” type roughness). A lithographic mask of various specimens (varying a and f) was created. The fabrication process was performed as

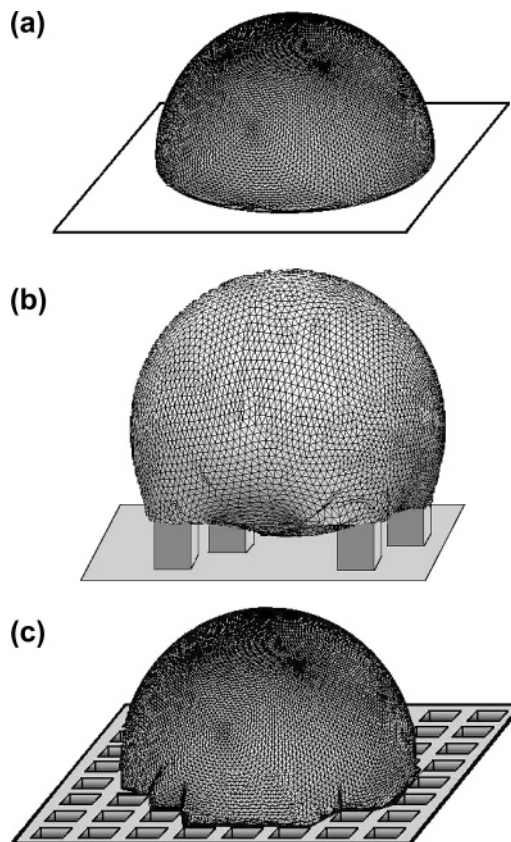


Figure 1. (a) Shape of a sessile drop on a smooth surface generated using Evolver.²⁶ (b) Shape of a sessile drop on a surface with square poles generated using Evolver.²⁶ (c) Schematic of a sessile drop on a surface with square holes.

follows: first, a 3” diameter $\langle 100 \rangle$ silicon wafer was cleaned using RCA1 and RCA2 cleans. Then, OCG-825 positive photoresist (Arch Chemicals, Inc., Norwalk, CA) was spin-coated at 3000 rpm for 40 s with a ramping rate of 200 rpm/s to obtain a 0.9 μm thick film. After soft baking at 95 $^\circ\text{C}$ for 30 min in a convection oven (National Compliance Co., Model 5831), a contact aligner MJB3 (Karl Suss, Germany) was used to expose the photoresist with a dose of 25 mJ/cm^2 at 405 nm exposure wavelength. This step was followed by developing (OCG Developer 934, diluted 2 parts of developer, one part of water for 65 s) and hard baking at 120 $^\circ\text{C}$ for 30 min in a convection oven (Fisher Isotemp Oven 200 Series Model 215F). The whole wafer was then etched using the deep reactive ion etching (DRIE) process in an Alcatel AMS 100 I-speeder DRIE system. The following recipe was used for the etching process: surface temperature, 10 $^\circ\text{C}$; helium pressure, 8.0 mbar; source power, 1800 W; gases, 300 sccm of SF_6 for 7 s, 150 sccm of C_4F_8 for 2 s; etch time, 6 min 40 s. Finally, the specimens were rendered hydrophobic by a silanization process identical to that used by Oner and McCarthy.³

Contact Angle Measurement. The advancing contact angles of a water drop on these samples were measured using a dynamic contact angle analyzer employing the captive needle technique (see, for example, He et al.⁹). For the purposes of this paper, the phrase “contact angle” will indicate the advancing contact angle, which is obtained as the asymptotic angle, while liquid is quasistatically injected into the drop. The contact angle measurement process was verified against the data of Oner and McCarthy³ for a plain silanized surface. The resulting data was also analyzed for repeatability and reproducibility. The uncertainty on the advancing angle for all the data presented herein was less than $\pm 1.5^\circ$.

Results and Discussion

Figure 3 is a graph of the advancing contact angle versus area void fraction (f) for a hole depth (or pole height) of D and side a . All the data reported in this figure is for $D = 30 \mu\text{m}$ for 20

(19) Marmur, A. Equilibrium contact angles: Theory and measurement. *Colloids Surf.* **1996**, *116*, 55–61.

(20) Ramos, S.; Tanguy, A. Pinning–depinning of the contact line on nanorough surfaces. *Eur. Phys. J. E* **2006**, *19* (4), 433–440.

(21) Extrand, C. W. Contact angles and hysteresis on surfaces with chemically heterogeneous islands. *Langmuir* **2003**, *19* (9), 3793–3796.

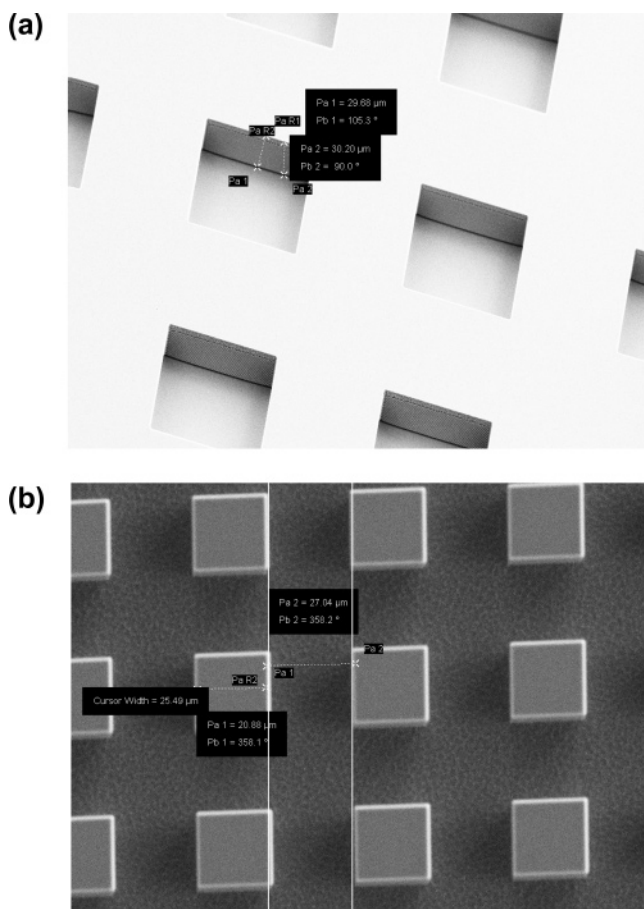


Figure 2. SEM image of the specimen with “holes” and “poles”.

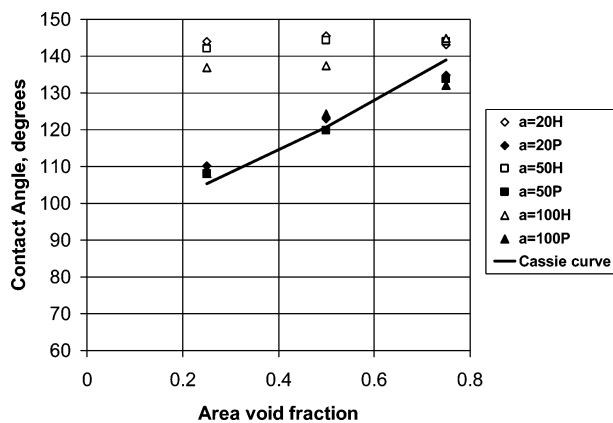


Figure 3. Contact angle versus area void fraction for varying characteristic lengths ($D = 30 \mu\text{m}$).

$\mu\text{m} \leq a \leq 100 \mu\text{m}$. For example, $a = 20\text{H}$ corresponds to data for a $20 \mu\text{m}$ square hole specimen (open symbols), while $a = 100\text{P}$ correspond to a $100 \mu\text{m}$ square pole specimen (solid symbols). It can be observed from Figure 3 that, for surfaces with periodically placed poles, the advancing contact angle of the water drop increases linearly with an increase in the area void fraction. The experimentally measured advancing contact angles are compared against predictions by the Cassie–Baxter theory in the same figure (see the solid line in Figure 3). The Cassie–Baxter theory predictions were calculated using eq 2, using the advancing contact angle for the smooth silanized specimen, which was measured to be 103° . The comparison between Cassie–Baxter theory and the advancing angle data in this figure results in a correlation coefficient R^2 better than 0.9. Such correlation

with Cassie–Baxter theory for poles has also been reported by other researchers.^{7,22}

The data presented in Figure 3 represents advancing contact angle measurements that were performed on samples with similar area void fractions and characteristic roughness length scales but varying in the three-phase contact line topology. For the purpose of this discussion, we define the three-phase contact line as comprising the set of points that are in contact with air, liquid, and solid. In the case of the specimen where the drop was sessile on a surface with square poles, the set of points forming the three-phase contact line is discontinuous, in effect amounting to the edges and tops of the square poles.

For the specimens with square cavities, the contact angle is seen to be independent of the area void fraction in Figure 3. Furthermore, it can be observed that the contact angles for the specimens with square cavities are greater than those of poles over the range of area void fractions investigated. Since the Cassie–Baxter theory does not distinguish between poles and cavities structures, this observed anomaly can possibly be attributed to the fundamental difference in the three-phase contact line topology—continuous for cavities and discontinuous for poles.

Recently, Gao and McCarthy²³ have debated that Cassie and Wenzel theory may not be on sound footing, owing to the experiments of Extrand²¹ and Bartell and Shepard²⁴ on islands of chemical heterogeneities. In their work, the contact line of the drop was on a locally homogeneous surface, whereas the drop surface areas were in contact with heterogeneous surfaces. In this paper, we present another novel situation in which we demonstrate departure from Cassie theory prediction. However, in the present work, the contact line experiences a heterogeneous surface and the Cassie theory is still violated. In addition, the length scale associated with the heterogeneity was comparable to the length scale of the drop in the experiments reported by Gao and McCarthy.²³ In contrast, we provide empirical evidence of a failure of Cassie theory even with surfaces whose heterogeneity length scale is much smaller than the length scale associated with the drop.

Conclusions

The contact angles were measured on various microstructured surfaces ranging in characteristic length scale as well as area void fraction. In particular, two types of surfaces consisting of square cross sectional poles and square cross sectional cavities were considered. The two types of surfaces differed mainly in the three-phase contact line topology of sessile drops placed on them. Conventional Cassie–Baxter theory¹² indicates that the area void fraction controls the resulting contact angle following Gibbs free energy minimization arguments²⁵ in both types of surfaces. In contrast, we found that the three-phase contact line topology may affect the dependence of the contact angle on the area void fraction. On surfaces with discontinuous three-phase contact line, the contact angle closely follows the prediction of the Cassie–Baxter theory, in agreement with results reported in the literature. However, for surfaces where the sessile drops exhibit a continuous three-phase contact line, the measured advancing angles are almost invariant with respect to the area void fraction.

(22) Bico, J.; Marzolin, C.; Quere, D. Pearl drops. *Europhys. Lett.* **1999**, *47* (2), 220–226.

(23) Gao, L.; McCarthy, T. J. How Wenzel and Cassie were wrong. *Langmuir* **2007**, *23*, 3762–3765.

(24) Bartell, F. E.; Shepard, J. W. Surface roughness as related to hysteresis of contact angle. II. The systems of paraffin–4 M–calcium chloride solution–air and paraffin–glycerol–air. *J. Phys. Chem.* **1953**, *57*, 455.

(25) Patankar, N. A. On the modeling of hydrophobic contact angles on rough surfaces. *Langmuir* **2003**, *19*, 1249–1253.

(26) Brakke, K. Personal communication. In Panchagnula, M. V., Ed. 2007.

Therefore, we conclude that the fundamental behavior of sessile drops on surfaces where the three-phase contact line is continuous is governed by other effects in addition to interfacial free energy minimization.

Acknowledgment. This work was partially supported by National Science Foundation (NSF) Major Research Instrumentation Grant ECS-0320659, through which DRIE equipment was

acquired by Lehigh University. We acknowledge the help of Mr. Wayne Kimsey with the data analysis and of Mr. Yi Yao with the sample fabrication. S.N. acknowledges the financial support of the DoE IAC program. We would like to thank Dr. Surya Ganti for helpful discussions and Prof. Ken Brakke for sharing the Evolver code.

LA702023E